Supplementary Information to:

Genomic and single-cell analyses reveal genetic signatures of swimming pattern and diapause strategy in jellyfish

Authors: Zhijun Dong[1,2]†*, Fanghan Wang[1,2]†, Yali Liu[2,3,4]†, Yongxue Li[1,2]†, Haiyan Yu[5], Saijun Peng[1,2], Tingting Sun[1,2], Meng Qu[2,3,4], Ke Sun[6], Lei Wang[1,2], Yuanqing Ma[7], Kai Chen[6], Jianmin Zhao[1,2]*, Qiang Lin[2,3,4]*

†Authors contributed equally to this work.

*Correspondence to: linqiang@scsio.ac.cn (Q.L.); zjdong@yic.ac.cn (Z.J.D.); jmzhao@yic.ac.cn (J.M.Z)

Affiliations:

[1]CAS Key Laboratory of Coastal Environmental Processes and Ecological Remediation, Yantai Institute of Coastal Zone Research, Chinese Academy of Sciences, Yantai, Shandong 264003, China.

[2]University of Chinese Academy of Sciences, Beijing 100101, China.

[3]CAS Key Laboratory of Tropical Marine Bio-Resources and Ecology, South China Sea Institute of Oceanology, Chinese Academy of Sciences, Guangzhou 510301, China.

[4]Guangdong Provincial Key Laboratory of Applied Marine Biology, South China Sea Institute of Oceanology, Chinese Academy of Sciences, Guangzhou 510301, China.

[5]College of the Environment and Ecology, Xiamen University, Xiamen 361102, China.

[6]State Key Laboratory of Primate Biomedical Research, Institute of Primate Translational Medicine, Kunming University of Science and Technology, Kunming, Yunnan 650500, China.

[7]Shandong Key Laboratory of Marine Ecological Restoration, Shandong Marine Resource and Environment Research Institute, Yantai, Shandong 264006, China.

Supplementary Information

Table of Contents

Supplementary Notes

Supplementary Note 1. Genome sequencing and assembly

The genome sequencing information of are presented in Supplementary Table 1, 2, and 4. We calculated and plotted the 17-mer depth distributions of *T. rubra* and *A. coerulea*; the results are presented in Supplementary Figure 2 and Supplementary Table 3. The statistics for the assembly steps are listed Supplementary Table 5. Benchmarking Universal Single-Copy Orthologs (BUSCOs) assessment showed that our assembly captured 92.4% and 86.4% of the complete BUSCOs of *T. rubra* and *A. coerulea*, respectively. For Hi-C sequencing, the sequence interaction matrices are shown in Supplementary Figure 3, and the statistical analysis results of the chromosome assembles of *T. rubra* (2n=30) and *A. coerulea* (2n = 44) with genomic loading rates of 95.11% and 99.71 %, respectively, are summarised in Supplementary Table 6 and 7 and schematic representation of the genomic characteristics are shown in Supplementary Figure 4. Furthermore, the pseudo-chromosome syntenic relationship between *T. rubra* and *A. coerulea* was analyzed (Supplementary Figure 5). Evaluation of the genome for completeness based on BUSCO resulted in values of 92.4% and 86.4%, respectively, indicating the high completeness and accuracy of the assembly (Supplementary Table 5).

Supplementary Note 2. Genome annotation

The results of genome annotation are summarized in Supplementary Table 8. We identified a total of 18,746 and 32,035 genes from *T. rubra* and *A. coerulea* genomes, respectively (Supplementary Table 9). In total, 90.14% and 97.13% of the predicted genes were annotated using different databases in *T. rubra* and *A. coerulea*, respectively (Supplementary Table 10). For annotation of non-coding RNAs (ncRNAs), microRNAs (miRNAs) and snRNAs were predicted using Rfam (v14.1), whereas tRNAs were screened using tRNAscan-SE (v1.3.1) and rRNA was predicted using BLASTN (v2.6.0) (Supplementary Table 11). The annotation results were evaluated using BUSCO (metazoa_odb10), and the results showed that our gene set contained 93.3% and 88.4% of complete ortholog genes of *T. rubra* and *A. coerulea*,

respectively (Supplementary Table 12), showing that our gene annotation was highly complete.

Supplementary Note 3. Phylogenetic analysis

To determine the phylogenetic positions of *T. rubra* and *A. coerulea*, phylogenetic analysis was conducted using whole-genome protein datasets of 17 cnidarians and one ctenophore as the outgroup. A stringent set of orthologues was identified. Alignment of these individual orthologous groups, followed by concatenation, resulted in amino acid alignment. Model prediction revealed that the JTTF model was the best-suited substitution model for concatenated alignment. RAxML was used to generate an ML tree for alignment using the best-fit model. The phylogenetic relationships between anthozoans, hydrozoans, cubozoans, and scyphozoans were consistent with those reported in previous studies based on molecular datasets. Our phylogenomic analysis also placed *T. rubra* within Hydrozoa and appeared to be a sister to *C. hemisphaerica*. The divergence times were estimated using the Markov chain Monte Carlo (MCMC) tree in PAML with calibration. Concatenated supergenes and species trees were used as input files.

Supplementary Note 4. Expansion and contraction of gene families

Gene expansion and contraction results for each branch of the phylogenetic tree were estimated. *T. rubra* harbored 81 significantly expanded and 278 significantly contracted gene families (Supplementary Figure 6, Supplementary Data 10). GO and KEGG enrichment analysis of contracted gene families in *T. rubra* were conducted by the GOseq R package and KOBAS software, respectively. A full list of the significantly enriched pathways is shown in Supplementary Data 11.

Supplementary Note 5. Gene loss

The lost gene families found in *R* language and manually searched are presented in Supplementary Data 12. A broader comparison of four vertebrates was conducted to confirm the number of genes or families associated with statocyst/otolith formation,

cilia, and nerves in compared species. GO and KEGG enrichment analysis of lost gene families in *T. rubra* were conducted by the GOseq R package and KOBAS software, respectively. All significantly enriched pathways are listed in Supplementary Data 13.

Supplementary Note 6. Positive selection of genes

A total of 548 PSGs were identified in *T. rubra* (FDR < 0.05) (Supplementary Data 1). The dN/dS valve was provided in the Supplementary Data 2. Notably, among these genes, we found several genes that play important roles in the statolith morphogenesis, ciliary movement, ciligenesis and some modulators that have been reported to be important for the statolith formation process (Supplementary Table 14). Genes involved in the nervous and muscular systems were also identified. GO and KEGG enrichment analyses were also conducted by the GOseq R package and KOBAS software. GO enrichment of positive selected genes (PSGs) in *T. rubra* is shown in Supplementary Data 3. Comparison of the amino acid substitutions of PSGs shown in Fig. 3b in different species were performed using MEGA-X v10.1.8, and sequences of four vertebrate species were obtained from NCBI, the GenBank accession numbers of these genes are listed in Supplementary Table 14.

Supplementary Note 7. Transcriptome analyses

The RNA sequencing information of two tissues (sensory organs and bell margins as controls) of four species (*C. quinquecirrha*, *R. esculentum*, *A. coerulea*, and *T. rubra*) is listed in Supplementary Data 4. Principal-component analysis (PCA) based on four species normalization genes of combined 32 transcriptomes suggested that there were more variations between species than between tissues (Supplementary Figure 7). DEGs in the tentacle bulbs of *T. rubra* with the rhopilia of the other three jellyfish were obtained using cross-species transcriptome comparisons of sensory organs (Supplementary Figure 8, Supplementary Data 5). GO and KEGG enrichment analysis of downregulated DEGs in *T. rubra* were conducted by the GOseq R package and KOBAS software, respectively. All significantly enriched pathways are listed in

Supplementary Data 6, and the top 20 significantly enriched GO terms for the downregulated DEGs in the tentacle bulb of *T. rubra* are shown for biological processes (BPs) and cellular components (CCs) in Supplementary Figure 9.

The DEGs information of the sensory organs compared with the control samples in each species is shown in Supplementary Figure 10, and 11, Supplementary Table 15 and Supplementary Data 7. The full list of significantly enrichment gene ontologies of the upregulated and downregulated DEGs in the sensory organs in each species (P-value <0.05) is shown in Supplementary Data 8. KEGG enrichment of cilium-related DEGs in the four jellyfish species (P-value<0.05) is shown in Supplementary Data 9.

Supplementary Note 8. RNAi experiment and RT-qPCR

The sequences of RNAi are provided in Supplementary Table 16. At the end of the RNAi experiment, polyps were observed, and the number of individuals at each stage of strobilation was recorded. The result is shown in Supplementary Figure 13a. The expression of target genes was assessed using RT-qPCR analysis, and the si-OM and si-LRR groups exhibited significant downregulation of gene expression, validating the efficacy of the siRNA treatment (Supplementary Figure 13b, $p < 0.001$; Supplementary Data 14). The RT-qPCR primer sequence of select gene are shown in Supplementary Table 17.

Supplementary Note 9. Variation of the transcriptional expression profile of hair, neural, and muscle cells between *T. rubra* and *A. coerulea*.

The sc-RNA sequencing information of *T. rubra* and *A. coerulea* medusa is listed in Supplementary Table 18. We generated cell atlas of medusa *T. rubra* and *A. coerulea* contain 22245 cells and 18936 cells, respectively, and the number of RNA detected and UMI per cell are shown in Supplementary Figure 14. The 18 putative cell clusters (associated markers in parentheses) with a resolution of 0.2 were assigned to 10 broad partitions and were annotated manually by combining analysis of underlying

molecular profiles and prior knowledge (Supplementary Figure 15; Supplementary Data 15). Stem/germ cells (*PCNA* and *NANOS*) were dominant in *T. rubra*, whereas glands (trypsin, chitinase, and *MUC2*) and nematoblasts (nematogalectin and *DKK3*) were dominant in *A. coerulea*. Gene expression in the hair cells of *T. rubra* and *A. coerulea* was compared and species-specific gene sets were clearly visualised. The DEGs in hair cells from *T. rubra* and *A. coerulea* are shown in Supplementary Data 16. GO enrichment analysis of the DEGs was conducted using the GOseq R package, and the full list of enriched terms is shown in Supplementary Data 17.

The list of different expressed genes (DEGs) in neural s and striated muscle between *T. rubra* and *A. coerulea* is shown in Supplementary Data 18 and 20, and GO enrichment terms are shown in Supplementary Data 19 and 21.

Supplementary Note 10. Single-cell transcriptional profiles of cyst (Cy) formation in *T. rubra*.

ScRNA-seq analysis was conducted on single cells sampled across five crucial life stages: medusa (Me), four-leaf structure (Ff), cyst (Cy), polyp (Po), and planula (Pl) (Supplementary Table 19). To facilitate comparative analyses across different developmental stages, we integrated the expression data from all libraries into a unified dataset and utilized the Harmony package (fast, sensitive, and accurate integration of single-cell data with Harmony) to mitigate batch effects. In total, we obtained a high-quality dataset comprising 44954 cells expressing 15478 genes, with a median of 668 genes per cell and 1521 unique molecular identifiers (UMIs) per cell, representing five critical stages of development. To construct a cell atlas, we performed a clustering analysis on the gene expression matrix, resulting in the identification of 36 distinct cell clusters. The cellular landscape was visualized using the uniform manifold approximation and projection (UMAP) technique. The 36 clusters were confidently assigned to six broad (associated markers in parentheses) cell types based on known markers and prior annotations (Fig. 5a), including stem/germ cells (*CNIWI*, *NANOS* and *PCAN*), gastroderm (*CTSZ* and *CTSB*),

epidermal/muscle cells (*MYHCKB* and *MYH2*), nematocytes (minicollagen and nematogalectin), neural cells (*SYT16* and neuocalcin), gland cells (chitinase 2 and *CELA3B*), and hair cell (myosin-VI, *MYO7A*, *PO4F3*). DEGs of *T.rubra* across different life stages are shown in Supplementary Data 25. The KEGG and GO enrichment analysess of cysts and planula in *T. rubra* (P-value < 0.05) are shown in Supplementary Data 23 and Supplementary Data 24, respectively.

Supplementary Note 11. Whole-mount in situ hybridisation protocol

Whole-mount in situ hybridised animals that had been starved for at least 2 days were relaxed in 2% $MgCl_2$ (in 0.22 µm filtered seawater) for 5–10 min and subsequently fixed overnight at 4 ℃ in 4% paraformaldehyde. Thereafter, the specimens were dehydrated using a 25/50/75% MeOH series to remove undesired pigmentation and stored in 100% MeOH at -20 ℃. The samples were rehydrated with a 75/50/25% MeOH series for 10 min each, followed by a 10-minute PBT wash, and then bleached in a 3% H2O2/PBT solution for 10 min. Animals were permeabilized for 10–20 min with 1 µg/ml proteinase K (Sigma) in PBT after three 10-min PBT washes. Protease digestion was stopped by a quick wash and a 10-min wash with 4 mg/ml glycine in PBT, followed by three 10-min PBT washes to remove residual glycine. The samples were washed twice with 0.1 M triethanolamine for 10 min, and then treated with 2.5 µl/ml and 5 µl/ml acetic anhydride in 0.1 M triethanolamine (pH 7.8) for 5 min each to reduce probe nonspecific binding. Hereafter, the samples were refixed overnight with 4% paraformaldehyde at 4 ℃.

The fixative was thoroughly washed with three 10-min PBT washes and two 10-min 2× SSC washes. The animals in 2× SSC were transferred to a 70 ℃ water bath for 20 min. Prehybridization and hybridization were all carried out in hybridization oven at 57 ℃. Prehybridization step was performed in hybridization buffer (50% Formamid, 5× SSC, 0.1% Tween-20, 0.1% CHAPS, 1× Denhardt's solution and 100µg/ml Heparin in DEPC water) with 0.5 mg/ml torula yeast RNA (Sigma; #R6625-25G) for 2 hours. For hybridisation, all probes denatured at 70 ℃ for

5 min were used at 10 ng/ml in hybridisation buffer with 0.5 mg/ml torula yeast RNA to improve signal-to-noise and hybridised for 24 hours with gentle agitation.

Unhybridized probes were washed away with pre-warmed solutions at 57 ℃ using 100% HS, 75% HS/25% 2× SSC, 50% HS/50% 2× SSC and 25% HS/75% 2× SSC for 10 min each, as well as 2× SSC with 0.1% CHAPS for two 30-min. This was followed by two 10-min washes with MAB-T (100 mM maleic acid, 150 mM NaCl, 0.1% Tween 20, pH 7.5). The samples were incubated in MAB-T with 1% BSA Fraktion V (Coolaber; # CA1381-10G) for 1 hour at RT, after which it was blocked at 4 ℃ for 2 hours in 1 ml blocking solution (80% MAB-T with 1% BSA and 20% sheep serum (Solarbio; #SL039)). The samples were incubated overnight with 1:2000 anti-DIG AP (Roche; #11093274910) in a blocking solution at 4 ℃.

The samples then were washed nine times with MAB-T for 20 min each, rinsed with NTMT (100 mM NaCl, 100 mM Tris-HCl, 50 mM MgCl2, and 0.1% Tween-20 in DEPC water, pH 9.5) for 10 min, and developed in the presence of NBT/BCIP substrate (Roche; #11175041910) at RT in the dark. The colour reaction was stopped by three PBT washes, and background staining was cleared by incubation in 70% and 100% EtOH. The samples were sequentially cleared with 80% glycerol. The primer sequences are listed in Supplementary Table 20.

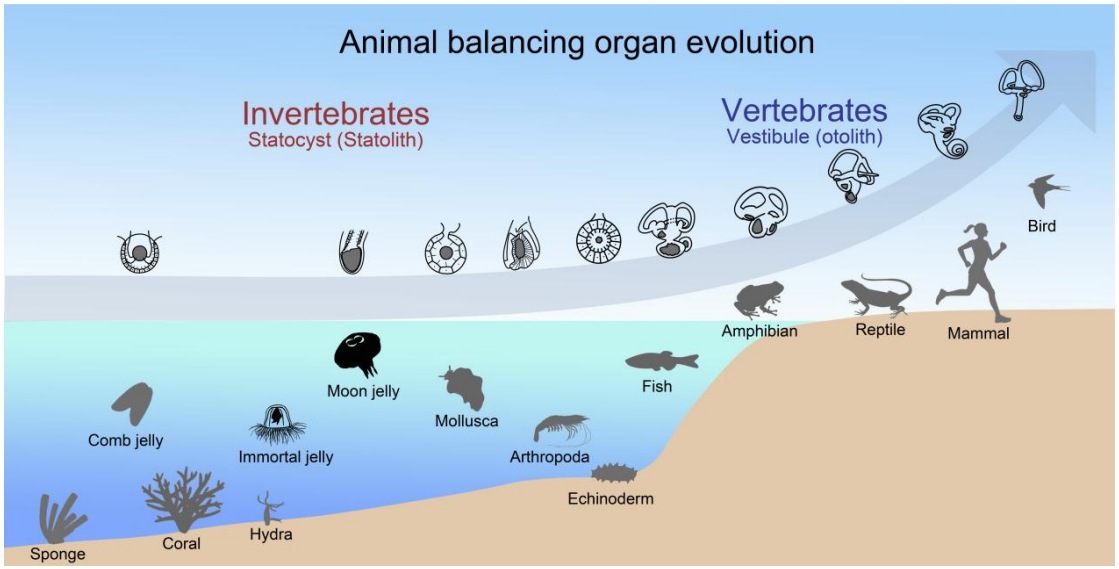

Supplementary Figure 1.

Balancing organs in Eumetazoa range from simple statocysts in aquatic invertebrates to complex vestibules in mammals, which comprise mass blocks of calcium crystals (statolith/otolith), proteoglycans and collagen, together with sensory hair cells mechanically influenced by the position of the mass blocks. The silhouette images of species were downloaded from BioRender. com except for echinoderm, hydra, immortal jelly and moon jelly.

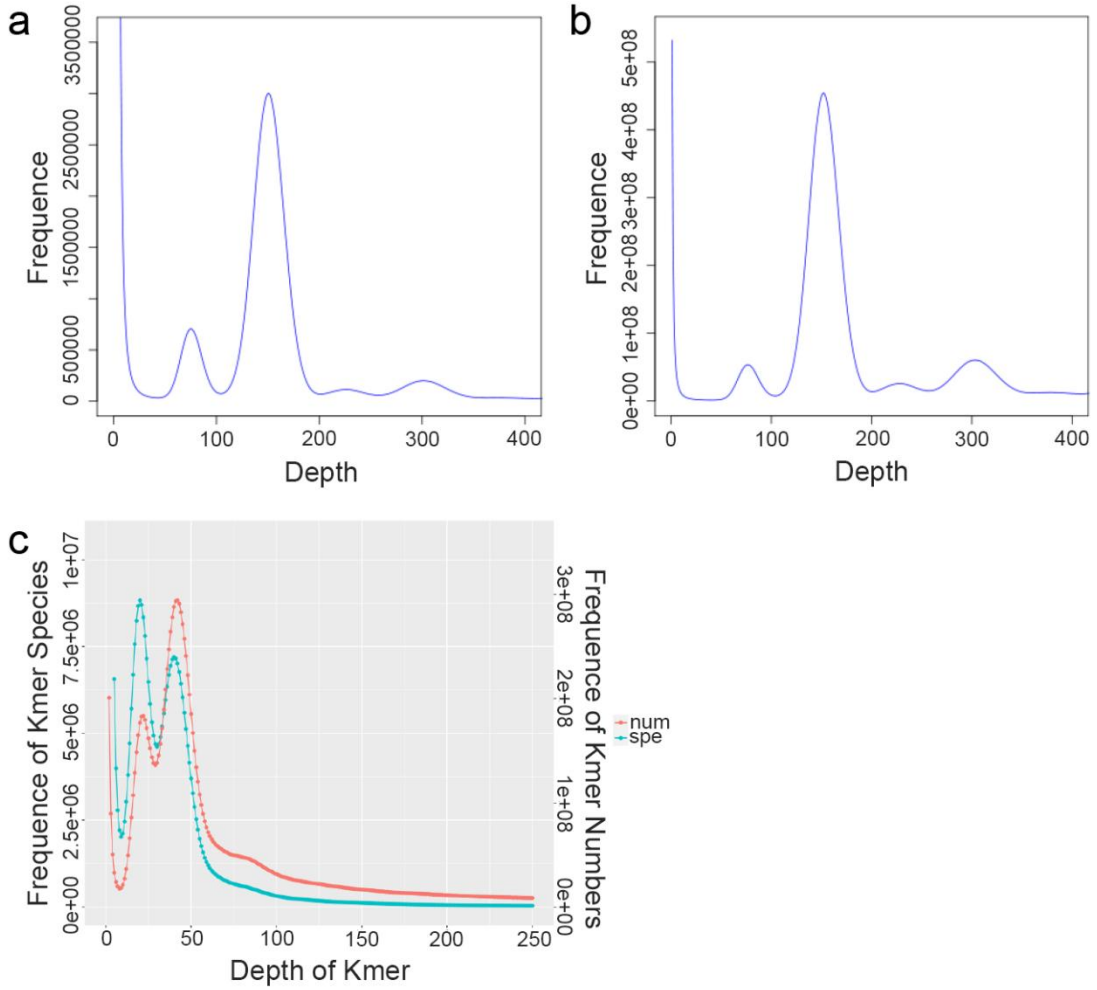

239

240 **Supplementary Figure 2.**

241 *K-mer* distribution of the *T.rubra* (a, b) and *A. coerulea* (c) genomes. The *K-mer*
242 spectrum was constructed based on a 17-*mer*. The figure shows the *K-mer* spectrum
243 of raw reads. The x-axis represents the *K-mer* depth, whereas the y-axis represents the
244 frequence of *Kmer* species (a, c) and numbers (b, c). The K*num* of the *T.rubra* and *A.*
245 *coerulea* genomes were 40,775,603,666 and 23130475928 based on the 17-mer. The
246 K*depth* were 151 and 40, respectively.

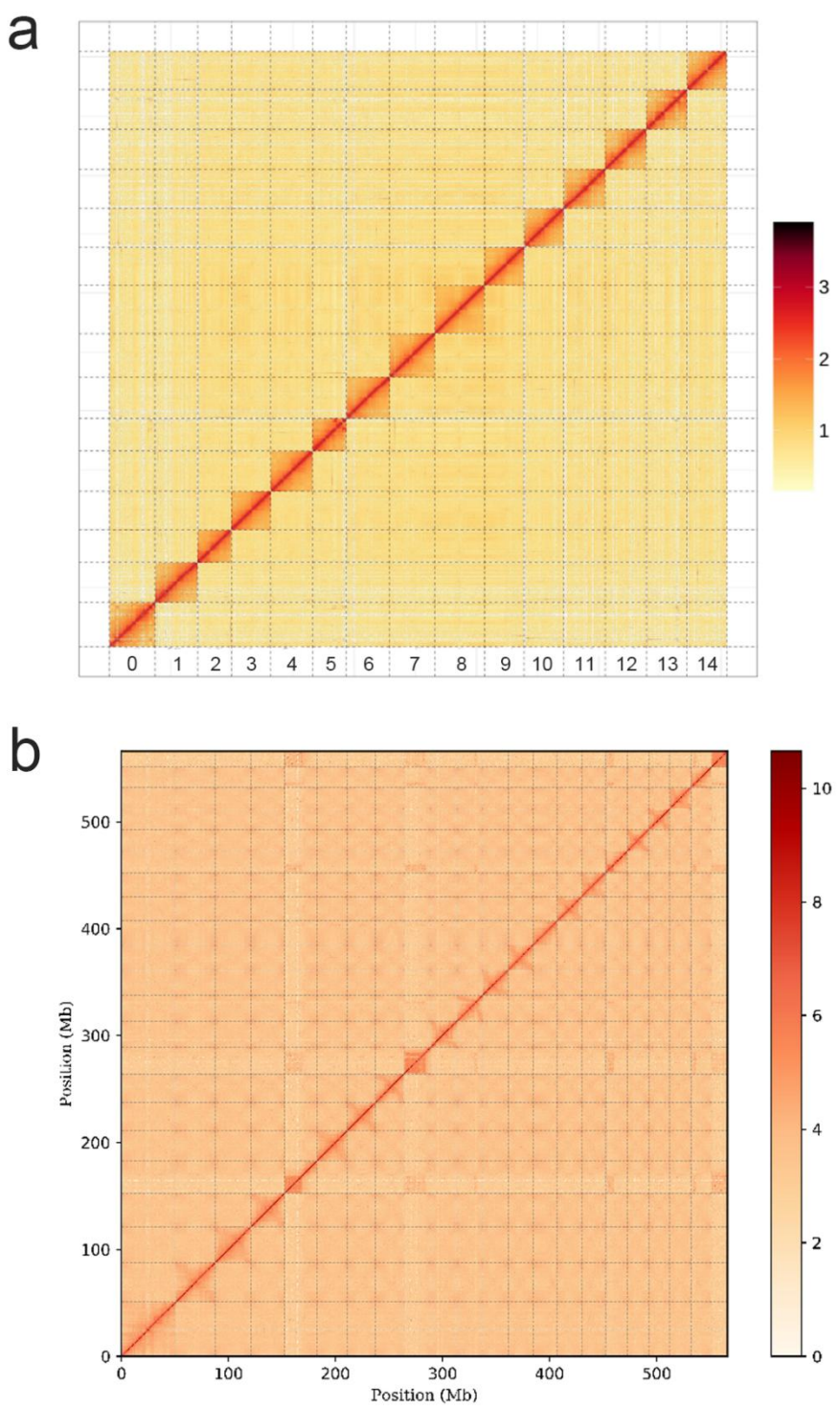

Supplementary Figure 3.

Hi-C contact maps of *T.rubra* (a) and *A. coerulea* (b) genome assemblies. Chromosome-level genome assemblies comprising 15 and 22 chromosome-level scaffolds, respectively.

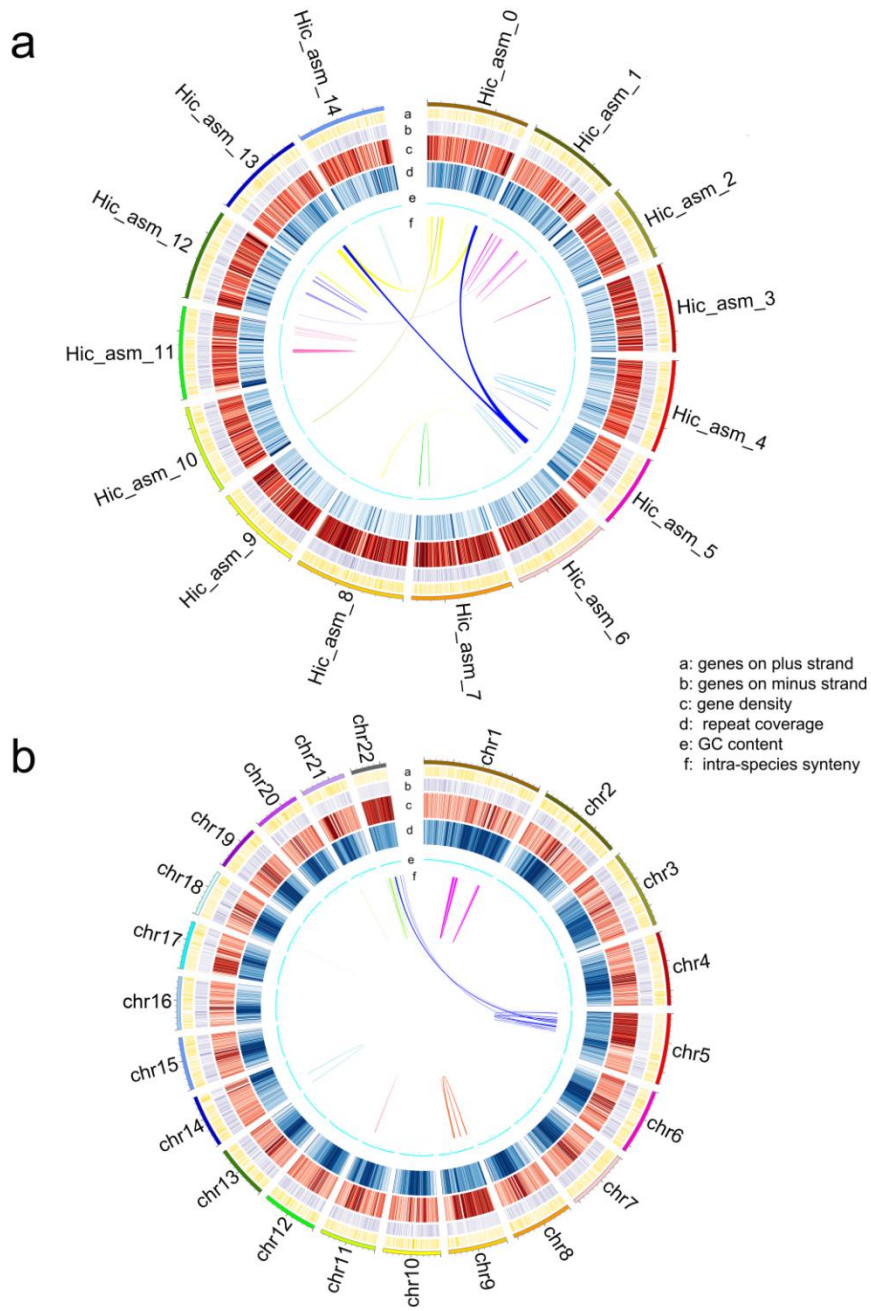

Supplementary Figure 4.

Schematic representation of the genomic characteristics of *T.rubra* (a) and *A. coerulea* (b). Track a: Proteincoding genes on plus strand. TrackB: Protein coding genes on minus strand. Track C: Distribution of gene density with sliding windows of 1 Mb. Higher density is shown in darker red colour. Track D: Distribution of GC content in the genome. Track E: Distribution of repeats in the genome. Track F: Schematic presentation of major interchromosomal relationships. Source data are provided as a Source Data file.

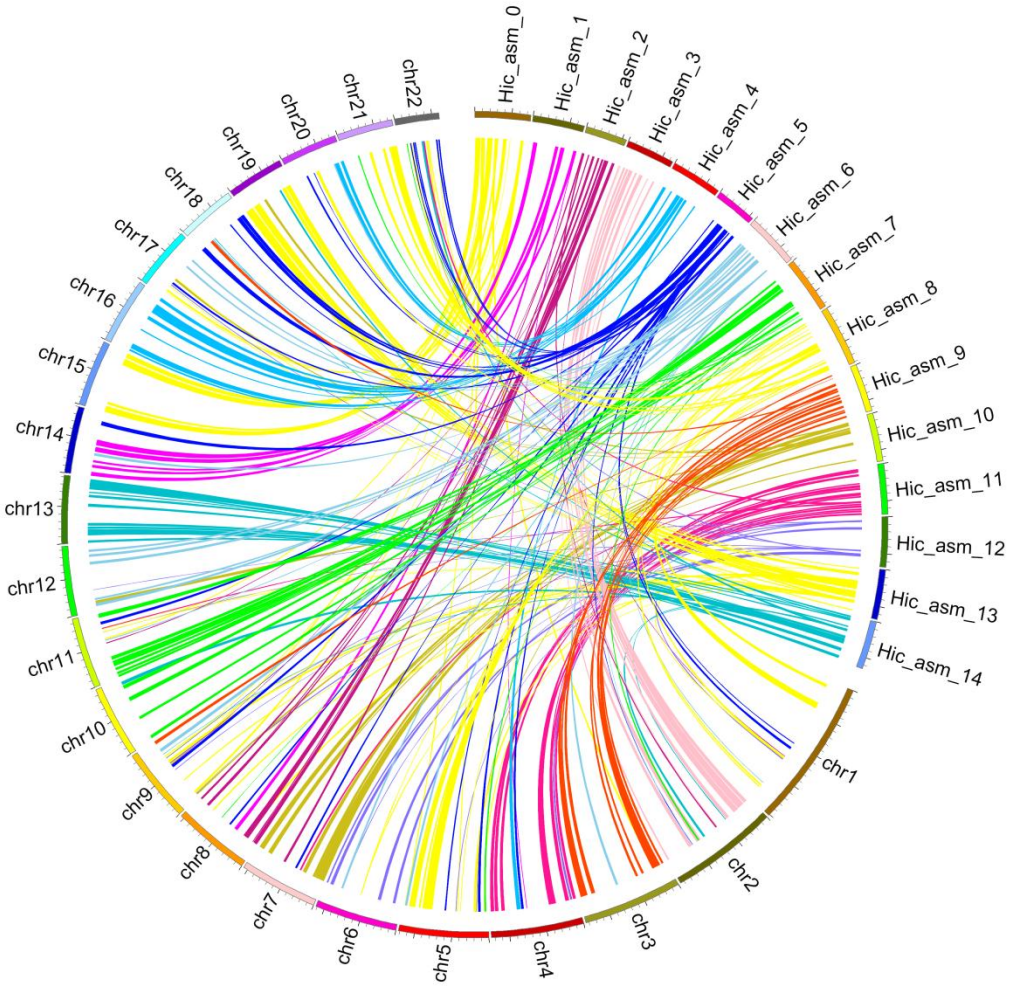

Supplementary Figure 5.

The chromosome synteny of *T. rubra* and *A. coerulea*. Source data are provided as a Source Data file.

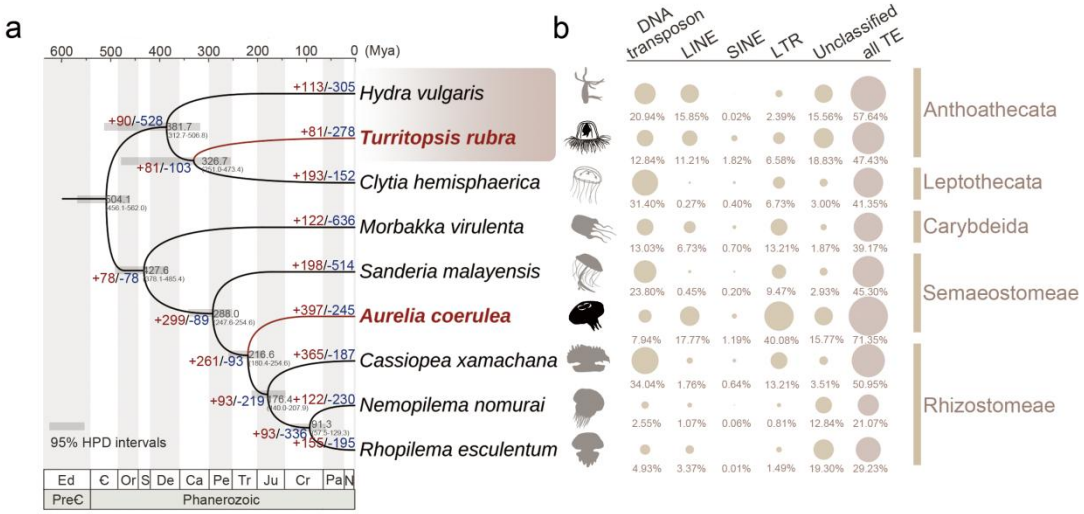

Supplementary Figure 6.

The numbers near each branch indicate the number of substantially expanded (red) and contracted (blue) gene families. *Hydra vulgaris* and *Turritopsis rubra,* which lack statocysts are presented in the red box. (b) Percentages of transposable elements (TEs) studied in the different jellyfish genomes studied. LINE, long interspersed element; SINE, short, interspersed element; LTR, long terminal repeats.

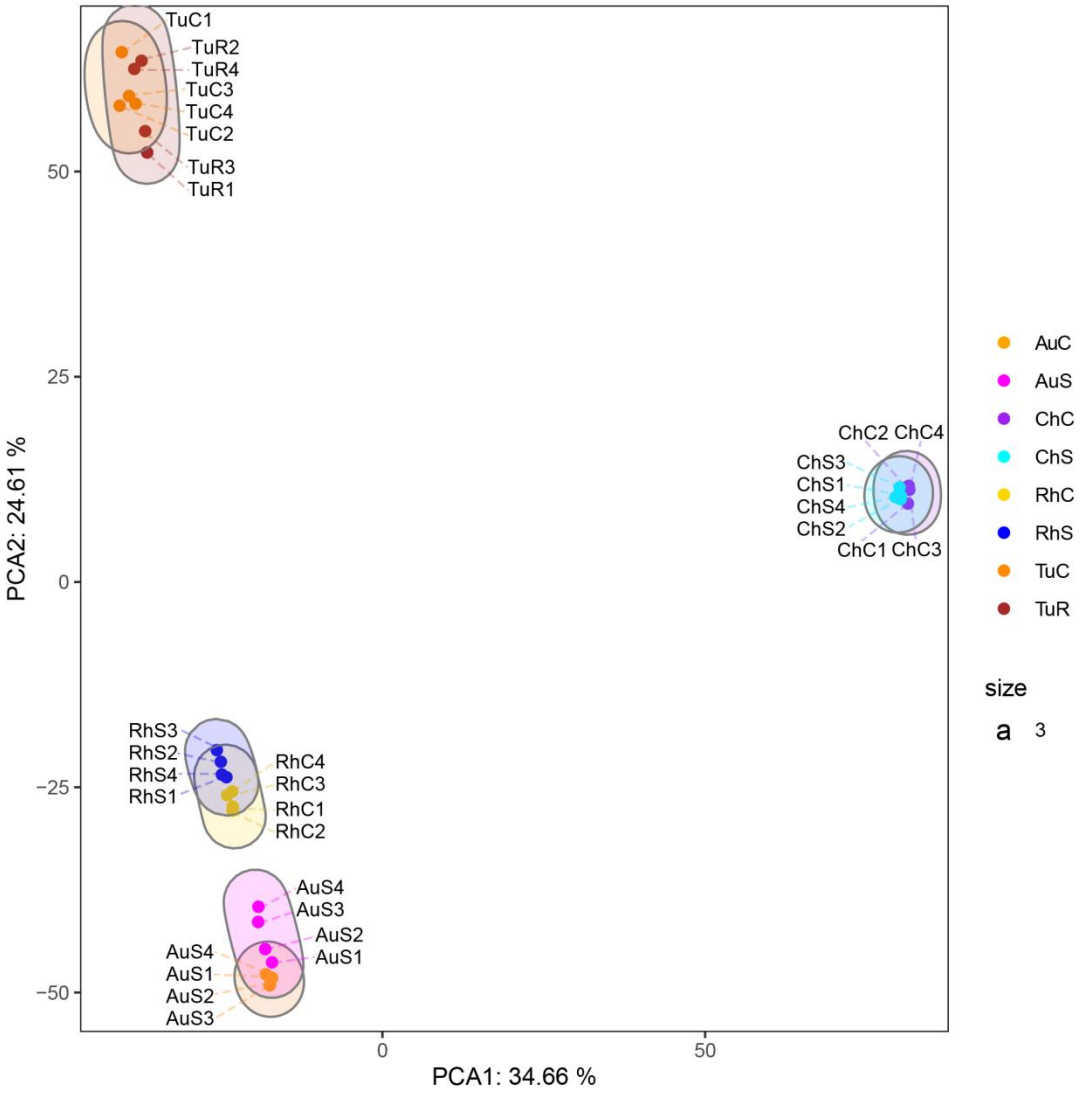

Supplementary Figure 7.

The principal-component analysis (PCA) clustered the 32 samples. The legend represents sample names in **Supplementary Table 15**. Source data are provided as a Source Data file.

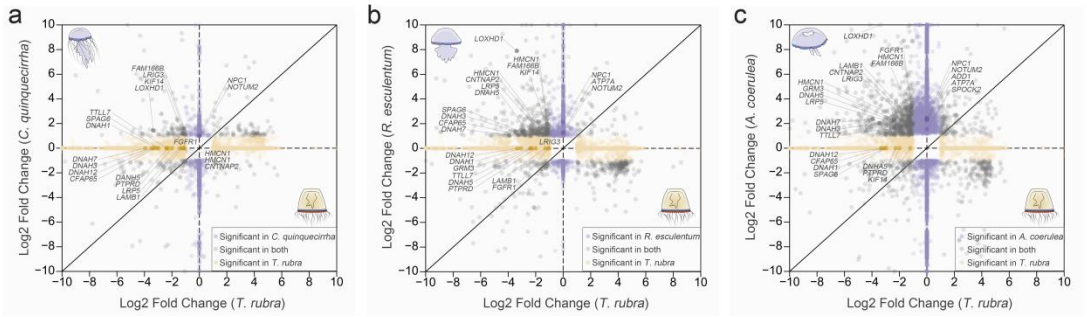

277

278 **Supplementary Figure 8.**

279 Volcano map of the shared and group-specific DEGs in the sensory organ and control
280 samples of *C. quinquecirrha* (a), *R. esculentum* (b) and *A. coerulea* (c) compared to
281 that in *T. rubra*. Yellow, purple and gray represent significantly changed DEGs in *T.*
282 *rubra*, scyphozoan and both groups, respectively. Source data are provided as a
283 Source Data file.

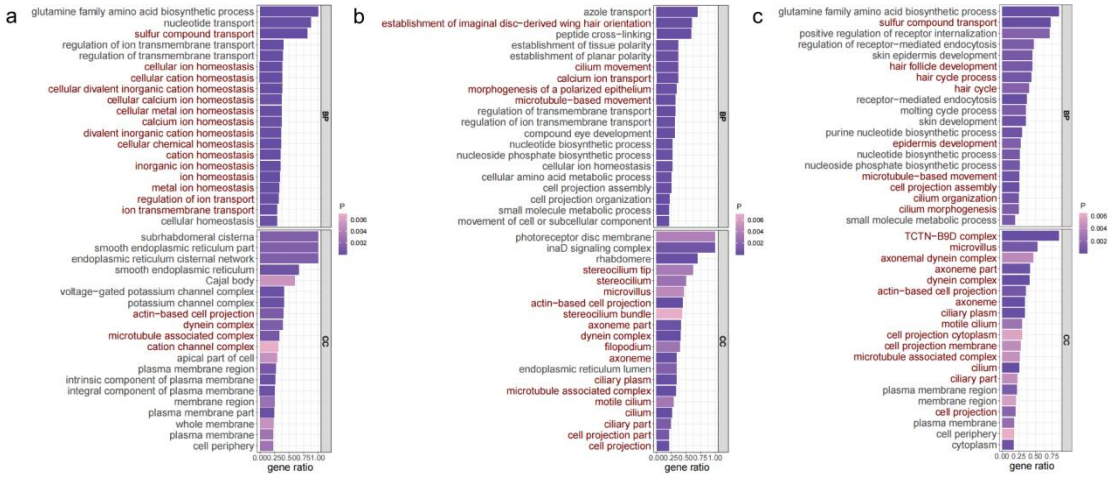

Supplementary Figure 9.

Top 20 enriched GO terms for downregulated DEGs in the tentacle bulb of *T. rubra* compared to three scyphozoan (a. *C. quinquecirrha*, b. *R. esculentum* and c. *A. coerulea*) are shown for biological processes (BPs) and cellular components (CCs). Categories involved in cilium are coloured in red. The enrichment was conducted using the GOseq R package and corrected $P < 0.05$ indicated significant enrichment. The complete categories are listed in Supplementary Data 6 ($P < 0.05$). Source data are provided as a Source Data file.

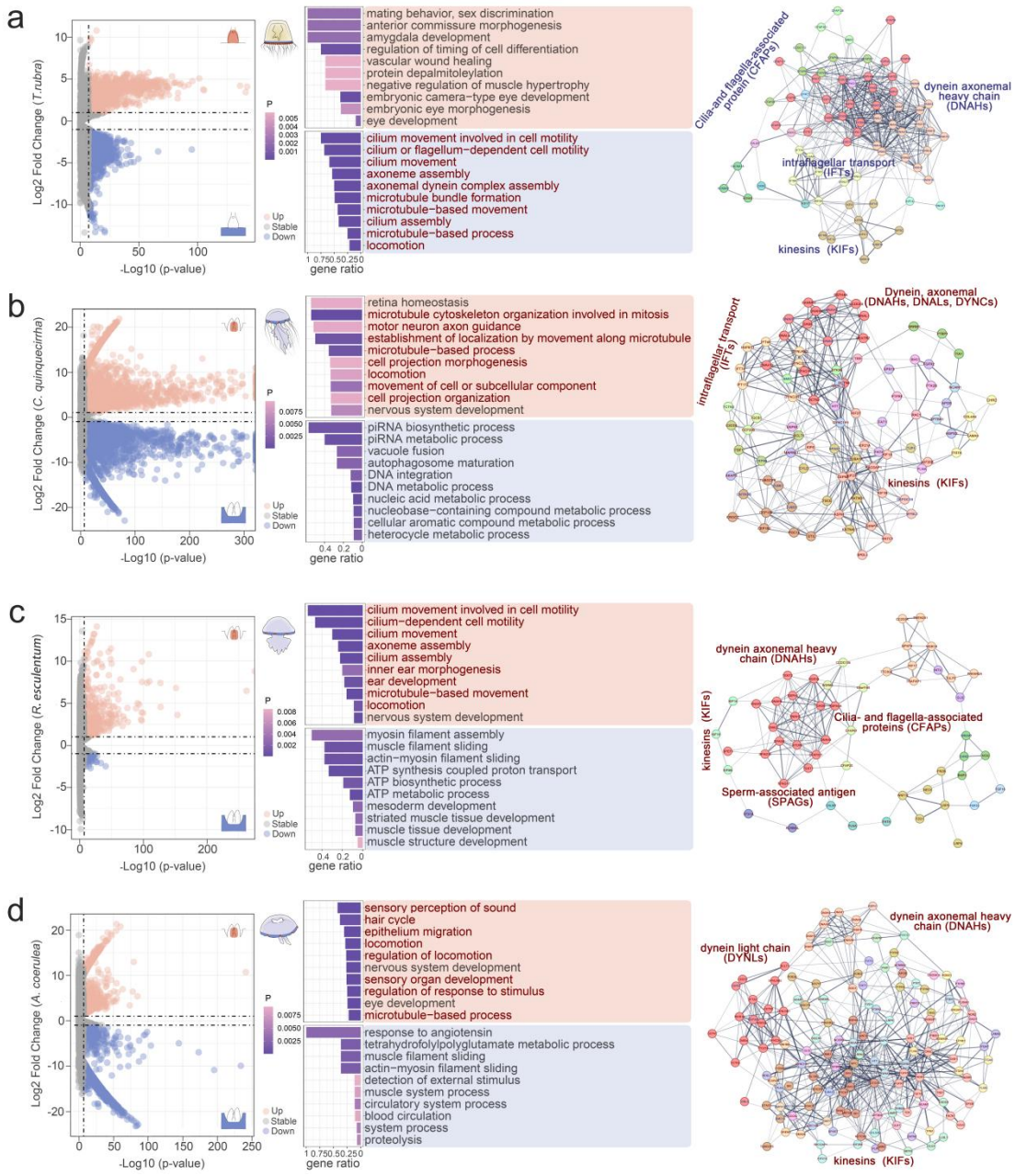

Supplementary Figure 10.

Volcano maps of differentially expressed genes (DEGs) in the sensory organs and control tissues of *Turritopsis rubra* (a), *Chrysaora quinquecirrha* (b), *Rhopilema esculentum* (c), and *Aurelia coerulea* (d), and significantly enriched Gene Ontology (GO) terms (biological processes, $p < 0.01$) of up-regulated and down-regulated DEGs in each species. Categories involved in cilium are coloured in red. The complete categories are listed in Supplementary Data 8 ($P < 0.05$). The interaction networks of cilium-related DEGs for each species are displayed in the right panel. The red and blue protein names in bubbles indicate up-regulated and down-regulated

proteins, respectively, in the sensory organ of each species. Edges represent protein–protein associations made using the STRING database with a medium confidence level (0.4). Coloured ellipses depict the regrouping of the closest clusters. The network of all the interactors was determined using Markov Clustering MCL (inflation parameter set to 3.0). Line thickness indicates the strength of evidence, with thicker connections representing higher confidence in the protein–protein interaction. Source data are provided as a Source Data file.

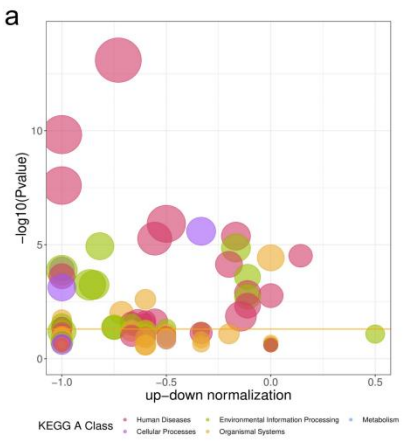

Pathway Top 20

ID	Descrption
ko05022	Pathways of neurodegeneration − multiple diseases
ko05016	Huntington disease
ko05014	Amyotrophic lateral sclerosis
ko05200	Pathways in cancer
ko04550	Signaling pathways regulating pluripotency of stem cells
ko05224	Breast cancer
ko05165	Human papillomavirus infection
ko04512	ECM−receptor interaction
ko04310	Wnt signaling pathway
ko05217	Basal cell carcinoma
ko04916	Melanogenesis
ko05226	Gastric cancer
ko04540	Gap junction
ko04151	PI3K−Akt signaling pathway
ko05032	Morphine addiction
ko04390	Hippo signaling pathway
ko04024	cAMP signaling pathway
ko04020	Calcium signaling pathway
ko04510	Focal adhesion
ko05225	Hepatocellular carcinoma

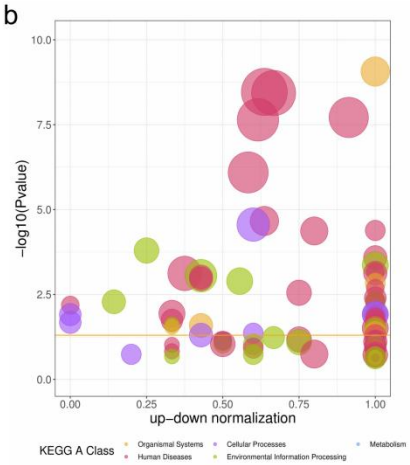

Pathway Top 20

ID	Descrption
ko04962	Vasopressin−regulated water reabsorption
ko05022	Pathways of neurodegeneration − multiple diseases
ko05014	Amyotrophic lateral sclerosis
ko05132	Salmonella infection
ko05016	Huntington disease
ko05200	Pathways in cancer
ko05224	Breast cancer
ko04510	Focal adhesion
ko05216	Thyroid cancer
ko05226	Gastric cancer
ko04350	TGF−beta signaling pathway
ko01521	EGFR tyrosine kinase inhibitor resistance
ko04013	MAPK signaling pathway − fly
ko05144	Malaria
ko01522	Endocrine resistance
ko05165	Human papillomavirus infection
ko04151	PI3K−Akt signaling pathway
ko05222	Small cell lung cancer
ko05146	Amoebiasis
ko04512	ECM−receptor interaction

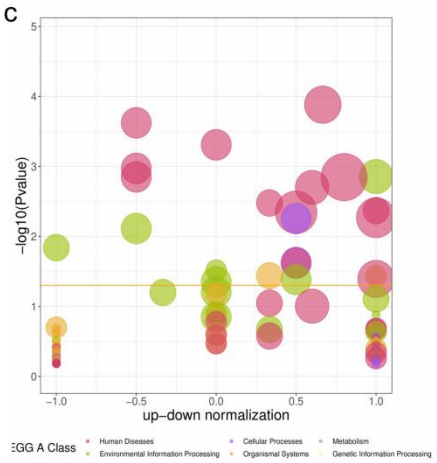

Pathway Top 20

ID	Descrption
ko05226	Gastric cancer
ko05416	Viral myocarditis
ko05412	Arrhythmogenic right ventricular cardiomyopathy
ko05410	Hypertrophic cardiomyopathy
ko04390	Hippo signaling pathway
ko05414	Dilated cardiomyopathy
ko05022	Pathways of neurodegeneration − multiple diseases
ko05224	Breast cancer
ko05218	Melanoma
ko05217	Basal cell carcinoma
ko05200	Pathways in cancer
ko05016	Huntington disease
ko04550	Signaling pathways regulating pluripotency of stem cells
ko04512	ECM−receptor interaction
ko04350	TGF−beta signaling pathway
ko04810	Regulation of actin cytoskeleton
ko05205	Proteoglycans in cancer
ko04016	MAPK signaling pathway − plant
ko04916	Melanogenesis
ko04911	Insulin secretion

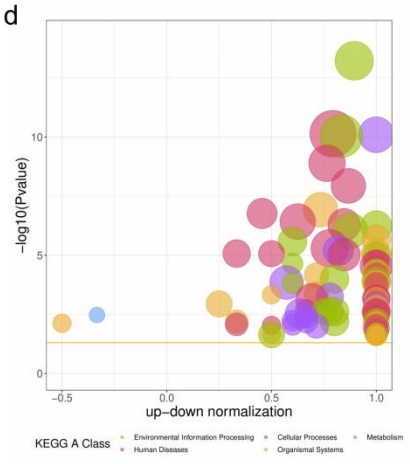

Pathway Top 20

ID	Descrption
ko04390	Hippo signaling pathway
ko05200	Pathways in cancer
ko04550	Signaling pathways regulating pluripotency of stem cells
ko04151	PI3K−Akt signaling pathway
ko05206	MicroRNAs in cancer
ko05226	Gastric cancer
ko04360	Axon guidance
ko05414	Dilated cardiomyopathy
ko05205	Proteoglycans in cancer
ko05224	Breast cancer
ko04391	Hippo signaling pathway − fly
ko04010	MAPK signaling pathway
ko04935	Growth hormone synthesis, secretion and action
ko04350	TGF−beta signaling pathway
ko05165	Human papillomavirus infection
ko04110	Cell cycle
ko05410	Hypertrophic cardiomyopathy
ko04722	Neurotrophin signaling pathway
ko05412	Arrhythmogenic right ventricular cardiomyopathy
ko05225	Hepatocellular carcinoma

310

Supplementary Figure 11.

Top 20 KEGG pathways for DEGs of the sensory organs and control tissues in *T. rubra* (a), *C. quinquecirrha* (b), *R. esculentum* (c) and *A. coerulea* (d). The complete categories are listed in Supplementary Data 9 ($P < 0.05$).

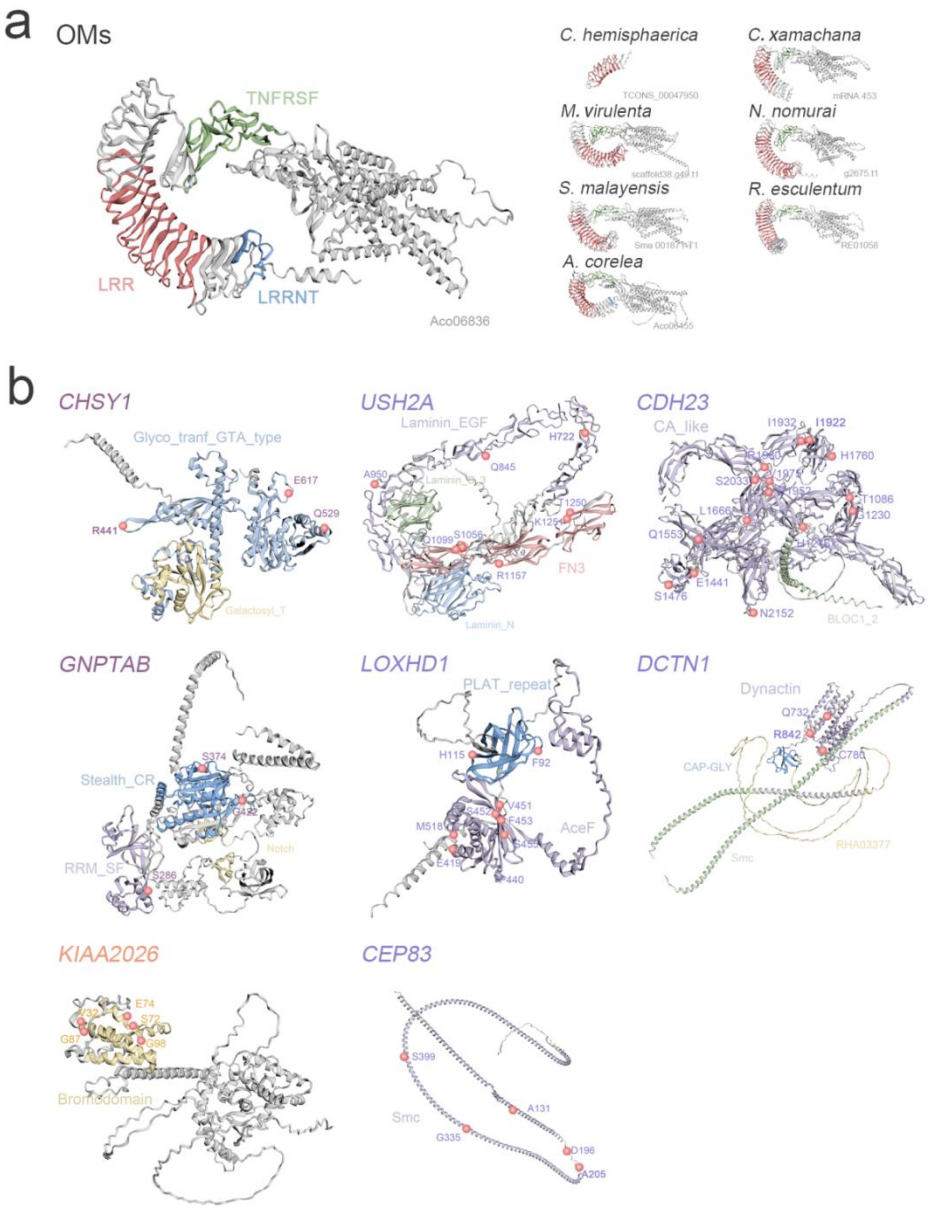

315

316 **Supplementary Figure 12.**

317 Predicted protein structures encoded by the lost otolith morphogenesis (OM) gene
318 family (a) and statocyst-related positively selected genes (PSGs) (b). (a) Predicted
319 protein structures encoded by OMs of each species revealed similar structures, with
320 an LRR (red) and TNFRSF (green) domains (except for *Clytia hemisphaerica*), in
321 addition to an LRRNT domain (blue) in front of the LRR in *Aurelia coerulea* and
322 *Rhopilema esculentum*. The LRR domain plays vital role in biomineralisation. (b)
323 Predicted protein structures encoded by some representing PSGs of Figure 2; selected
324 amino acids are labelled on conserved domains, which are represented in different
325 colours.

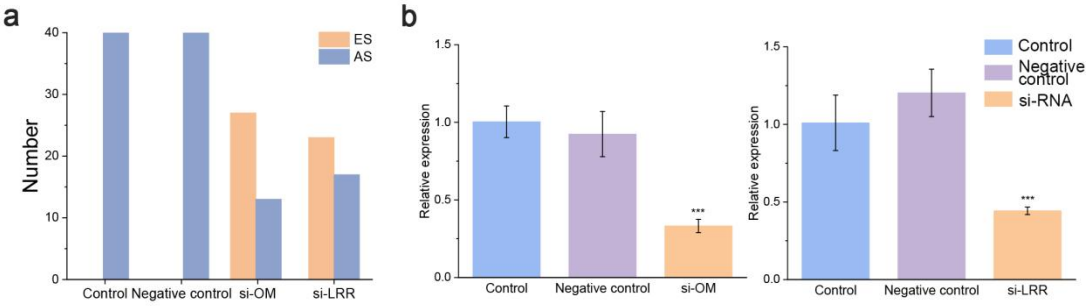

Supplementary Figure 13.

(a) The number of polyps under two stages of four groups. ES, early stage of strobilation; AS, advanced stage of strobilation. (b) The relative expression of target genes in the si-OM and si-LRR groups. Source data are provided as a Source Data file.

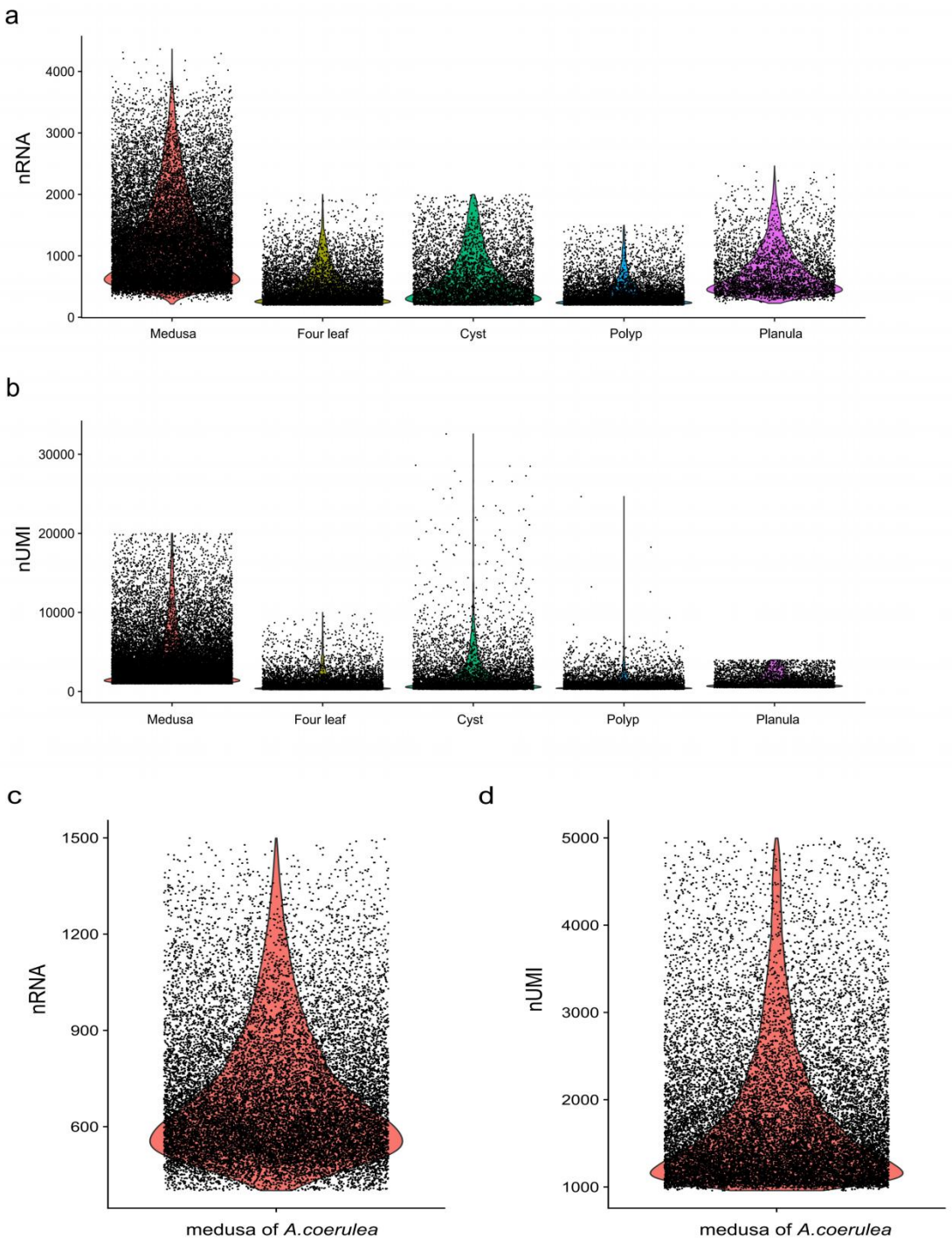

332

333 **Supplementary Figure 14.**

334 Violin plot showing the number of RNA detected (top) and UMI (bottom) per cell of

335 different life stage in *T.rubra* (a, b) and medusa of *A.coerulea* (c, d).

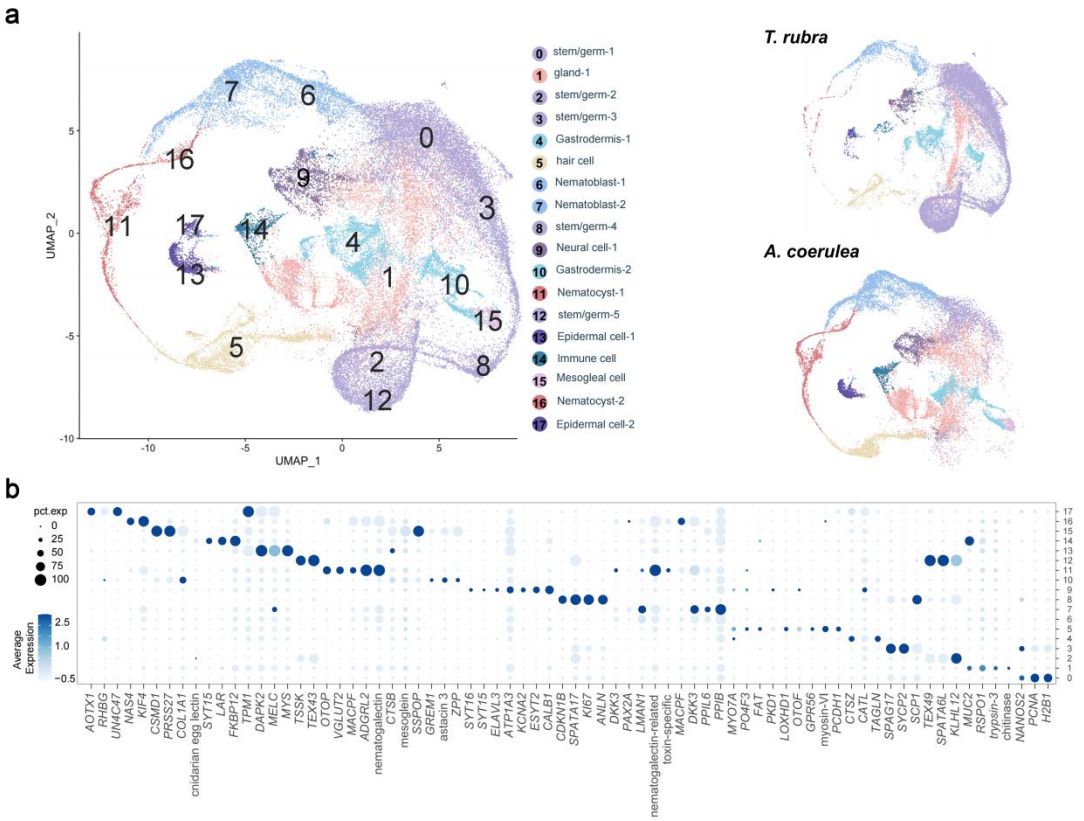

Supplementary Figure 15.

Cell atlas of the *T. rubra* and *A. coerulea*. (a) UMAP visualization of the merged dataset (left) and each life stage (right). coloured by cluster identity from Louvain clustering and annotated based on marker genes, cell-type colours are the same in each life stage, associated with **Figure 4**. (b) Dot plot showing expression of selected marker genes per cell type. Dot sizes represent percentages of cells within a cell type in which a given marker is detected; dot intensities represent average expression levels.

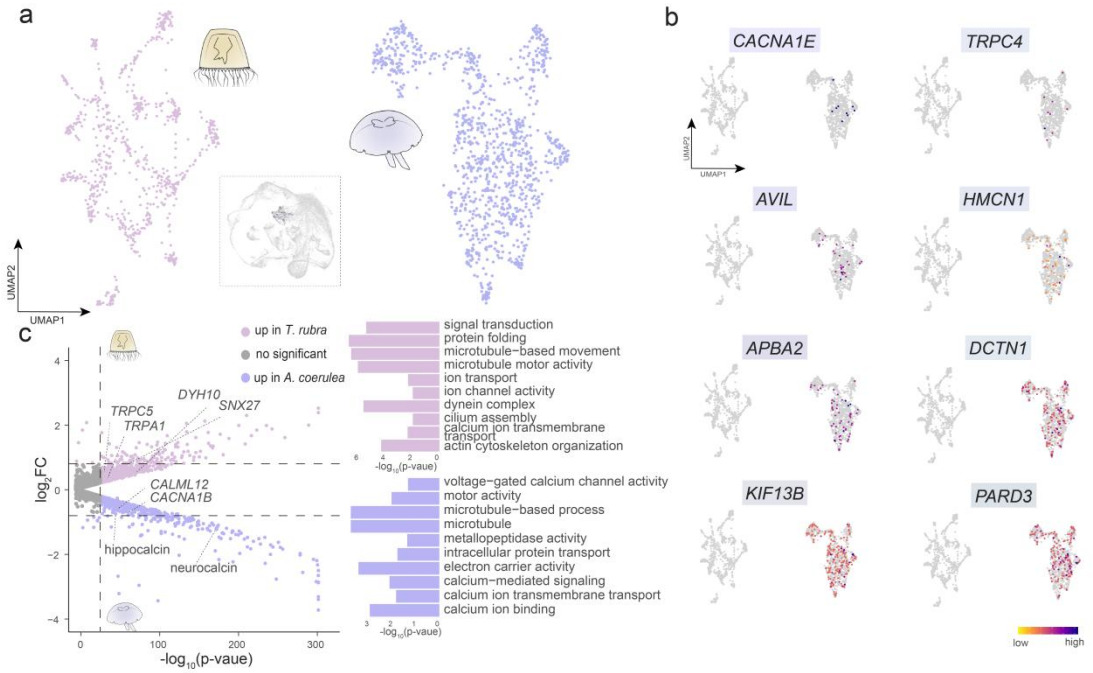

Supplementary Figure 16.

Cross-species comparison of neural cells in *Turritopsis rubra* and *Aurelia coerulea.* (a) Uniform Manifold Approximation and Projection (UMAP) visualisation of neural cells in the *T. rubra* and *A. coerulea* integrated medusa cell atlas. Inset: locations of the neural cell cluster of the merged UMAP plot in Figure 4a. (b) Feature plots visualising the expression of genes associated with neural development in neural cells. (c) Volcano map (left) displaying differential gene expression between the neural cells of *T. rubra* and *A. coerulea*; bar plot (right) depicts Gene Ontology (GO) analyses for differentially expressed genes (DEGs). Source data are provided as a Source Data file.

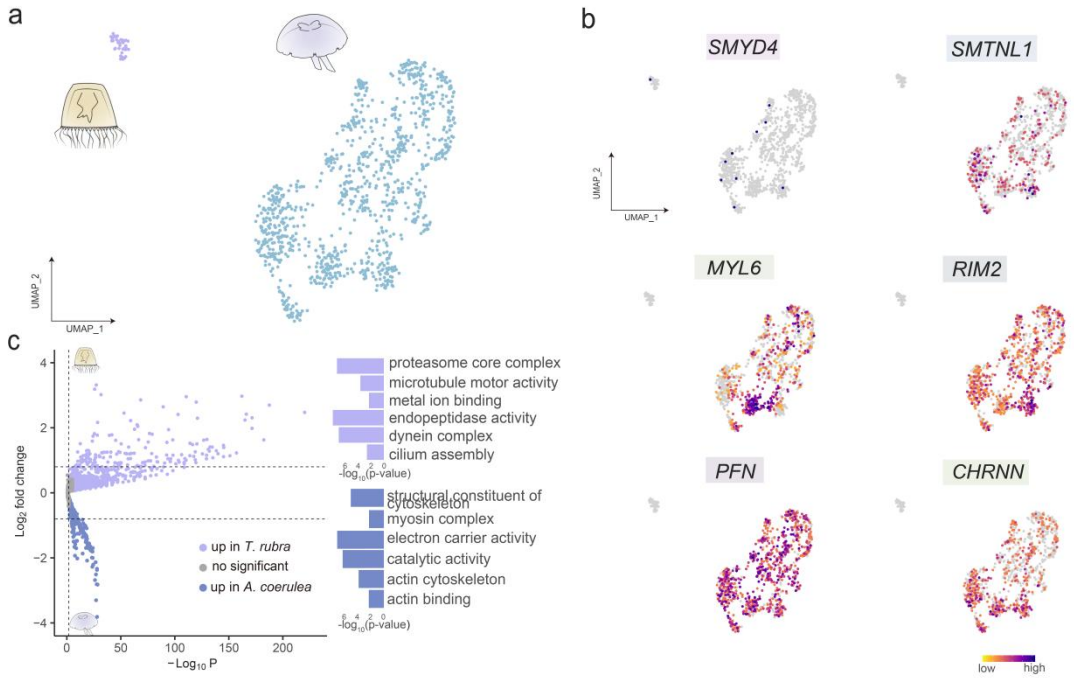

Supplementary Figure 17.

Cross-species comparison of striated muscle cells between *Turritopsis rubra* and *Aurelia coerulea* (a) Uniform Manifold Approximation and Projection (UMAP) visualisation of striated muscle cells in the *T. rubra* and *A. coerulea* integrated medusa cell atlas. (b) Feature plots showing the expression of genes associated with muscle contraction in striated muscle cells. (c) Volcano plot (left) depicting the differential gene expression between striated muscle cells of *T. rubra* and *A. coerulea*; bar plot (right) represents the Gene Ontology (GO) analyses for differentially expressed genes (DEGs). Source data are provided as a Source Data file.

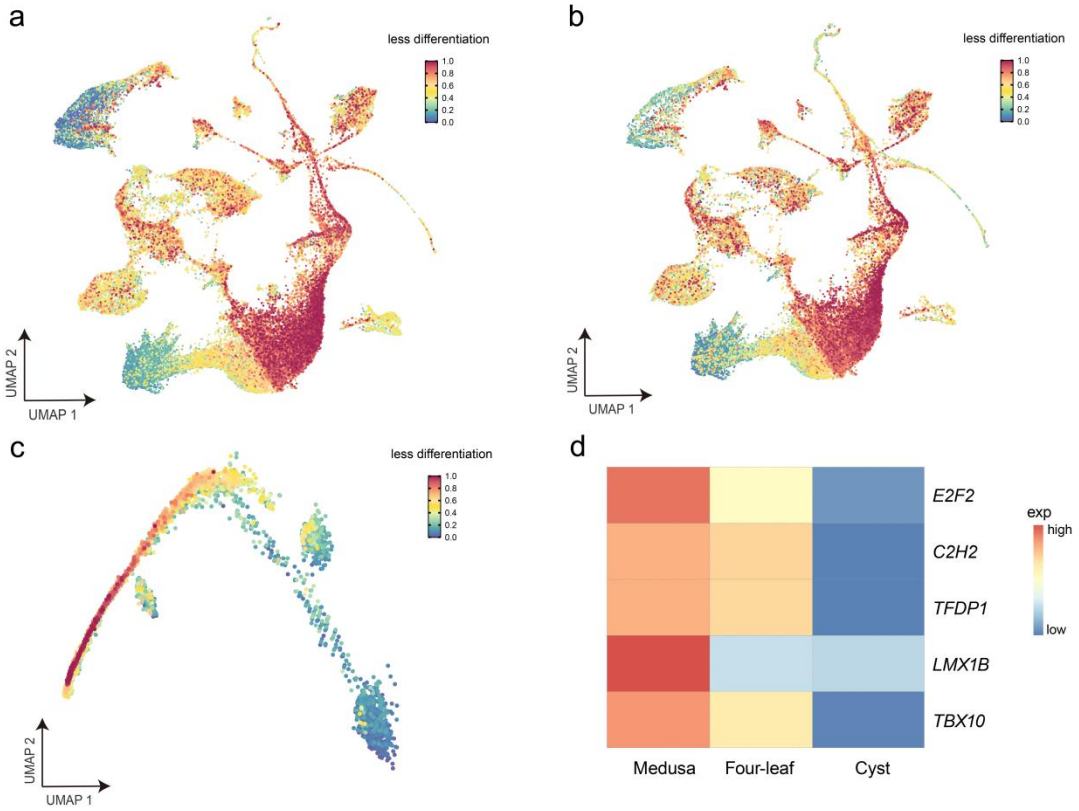

Supplementary Figure 18.

Analyses of the cell differentiation trajectory at different stages in *T. rubra*. (a-b) UMAP visualisation of the cell differentiation potential during the normal development stage (a) and the reverse-development stage (b) of the *T. rubra*. (c) Dynamics of differentiation potential between stem cells and nematocytes during the forward development process in *T. rubra*. (d) Heatmap showing the expression dynamics of selected transcription factors related to nematocyte differentiation during reverse development in *T. rubra*, related to Figure 5c. Source data are provided as a Source Data file.

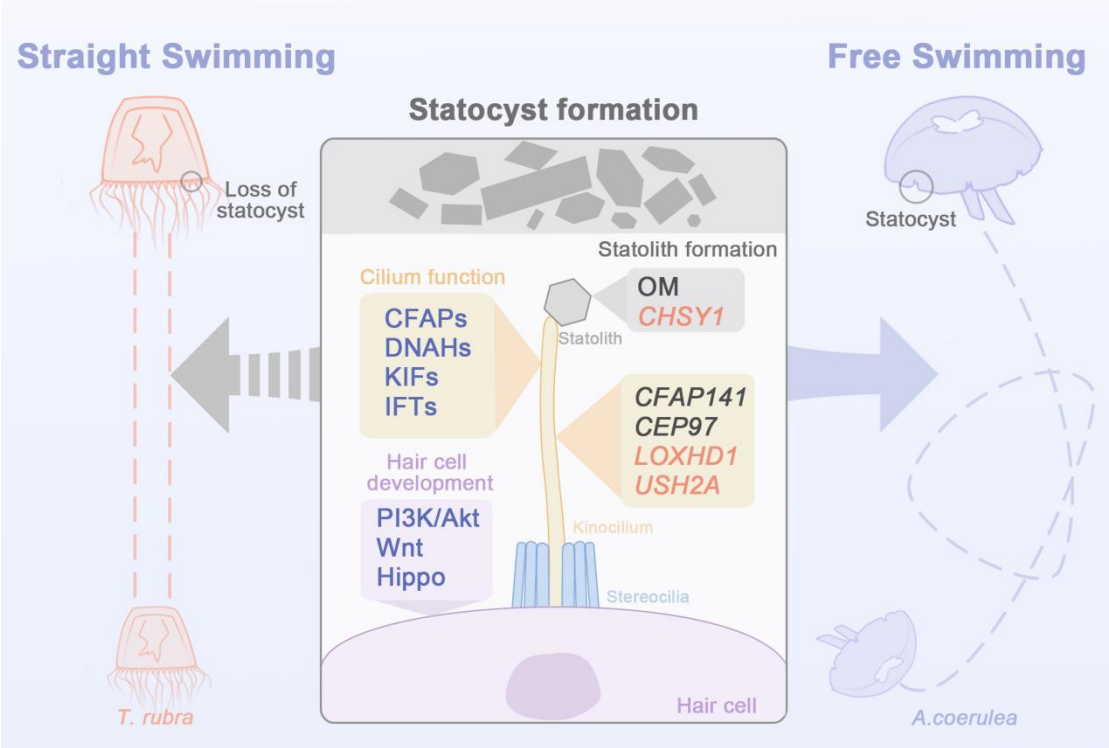

Supplementary Figure 19.

Genetic basis for the swimming patterns of *T. rubra* and *A. coerulea*. Lost genes (grey), positively selected genes (orange), and down-regulated or non- expressed genes and pathways (blue) in the hair cells of *T. rubra*, which are related to statocyst formation and cilium function and may result in the loss of statocyst and straight-swimming patterns in *T. rubra*.

Supplementary Table 1. Jellyfish samples used for genome and Hi-C sequencing.

Species Sampling	Origin	Sampling date	Genome sequencing	Hi-C sequencing	Note
T. rubra	Yantai and Dongying, Shandong, China	2021.6.5	individual	individual	newly sequenced
A. coerulea	Yantai, Shandong, China	2021.12.4	individual	individual	newly sequenced

Supplementary Table 2. Genome sequencing data by Illumina.

Sample ID	Library	Data (Gb)	Depth
T. rubra	350bp	53.43	200×
A. coerulea	350bp	60.90	120×

Supplementary Table 3. **Genome size estimation with *K-mer* distribution analysis based on a 17-*mer*.**

Sample ID	Genome size (Mb)	Heterozygosity (%)	Repeat ratio (%)
T. rubra	266.51	0.45	48.17
A. coerulea	521.62	1.43	56.18

Supplementary Table 4. Sequencing data evaluation for Hi-C assemblies.

Species	Raw paired reads	Raw Base(bp)	Clean Base(bp)	Q20(%)	Q30(%)	GC Content(%)
T. rubra	12,317,885	3,695,365,500	3,685,032,300	97.23	91.97	35.80
A. coerulea	461,577,177	68,707,838,179	68,315,728,511	98.80	95.70	37.30

Supplementary Table 5. Summary of genome sizes and assembly statistics.

Species Genome size	Assembly size (bp)	Scaffold num	Scaffold N50(bp)	Contig num	Contig N50 (bp)	Complete BUSCOs (%)	Fragmented BUSCOs (%)	Missing BUSCOs (%)	Loading rate (%)
T. rubra	266,862,699	329	16,943,197	762	1,187,606	92.40	1.30	6.30	95.11
A. coerulea	566,061,810	321	25,260,120	42	22,395,985	86.40	6.80	7.20	99.71

Supplementary Table 6. Statistics of the anchored chromosomes for *T. rubra* genome.

	Sequeues ID	Cluster Number	Sequeues Length
T. rubra	Hic_asm_0	57	18,799,587
	Hic_asm_1	42	17,348,683
	Hic_asm_2	19	13,911,814
	Hic_asm_3	15	16,302,533
	Hic_asm_4	20	17,136,266
	Hic_asm_5	27	13,858,914
	Hic_asm_6	24	17,883,988
	Hic_asm_7	20	18,556,697
	Hic_asm_8	13	20,379,689
	Hic_asm_9	16	16,246,515
	Hic_asm_10	30	16,356,653
	Hic_asm_11	35	17,031,648
	Hic_asm_12	36	16,943,197
	Hic_asm_13	46	16,806,440
	Hic_asm_14	48	16,243,415

Supplementary Table 7. Statistics of the anchored chromosomes for *A.coerulea* genome.

	Superscaffold	Number of Contigs	Length of Contigs	Length of Superscaffold
A.coerulea	chr1	4	50,743,788	50,745,288
	chr2	1	36,548,555	36,548,555
	chr3	4	33,598,094	33,599,594
	chr4	4	31,316,877	31,318,377
	chr5	1	30,607,789	30,607,789
	chr6	1	28,066,466	28,066,466
	chr7	1	26,734,379	26,734,379
	chr8	1	26,296,151	26,296,151
	chr9	2	25,259,620	25,260,120
	chr10	1	24,443,289	24,443,289
	chr11	2	24,105,683	24,106,183
	chr12	1	23,738,836	23,738,836
	chr13	2	23,151,249	23,151,749
	chr14	4	22,688,858	22,690,358
	chr15	2	22,541,530	22,542,030
	chr16	1	22,395,985	22,395,985
	chr17	1	20,565,505	20,565,505
	chr18	1	20,011,490	20,011,490
	chr19	1	19,548,997	19,548,997
	chr20	3	19,537,659	19,538,659
	chr21	2	19,094,960	19,095,460
	chr22	2	15,066,050	15,066,550

Supplementary Table 8. Statistics of TEs in *T. rubra* and *A.coerulea* genomes.

Species	Type	Denovo+Repbase Length(bp)	Rate (%)	TE proteins Length(bp)	Rate (%)	Combined TEs Length(bp)	Rate (%)
T. rubra	DNA	30,634,570	11.48	11,144,987	4.18	34,270,163	12.84
	LINE	25,796,510	9.67	11,973,960	4.49	29,915,257	11.21
	SINE	4,869,953	1.82	0	0.00	4,869,953	1.82
	LTR	16,260,095	6.09	2,939,498	1.10	17,550,578	6.58
	Other	0	0.00	0	0.00	0	0.00
	Unknown	50,261,822	18.83	0	0.00	50,261,822	18.83
	Total	120,603,297	45.19	25,944,876	9.72	126,581,914	47.43
A.coerulea	DNA	45,886,648	7.97	707,009	0.12	45,727,839	7.94
	LINE	96,396,367	16.75	20,206,690	3.51	102,296,994	17.77
	SINE	6,859,988	1.20	0	0.00	6,853,467	1.19
	LTR	232,566,099	40.41	9,031,961	1.57	230,701,339	40.08
	Other	0	0.00	0	0.00	0	0.00
	Unknown	90,804,249	15.77	0	0.00	90,778,823	15.77
	Total TE	408,176,930	70.92	29,940,888	5.20	410,702,814	71.35

403 **Supplementary Table 9. Statistics of the gene prediction in *T. rubra* and**
404 ***A.coerulea*.**

Species	Gene set	Software	Species	Number
T. rubra	*De novo*	Augustus	-	16,812
		GlimmerHMM	-	27,384
		SNAP	-	22,730
		Geneid	-	5,765
		Genscan	-	12,883
	Homolog	Blast and Genewise	*Aurelia aurita*	20,506
			Clytia hemisphaerica	25,304
			Hydra vulgaris	17,557
			Morbakka virulenta	15,451
			Pocillopora damicornis	18,625
			Rhopilema esculentum	21,438
	RNAseq	PASA	-	48,492
		Cufflinks	-	46,749
	Intergration	EVM	-	18,746
A.coerulea	*De novo*	Augustus	-	51,133
		Genscan	-	49,597
		GlimmHMM	-	79,009
	Homolog	Exonerate	*Aurelia aurita*	76,379
			Aurelia sp1	86,080
			Cassiopea xamachana	36,171
			Chrysaora quinquecirrha	37,770
			Hydra vulgaris	17,611
			Rhopilema esculentum	32,353
	RNAseq	PASA	-	6,658
	Intergration	MAKER	-	32,035

Supplementary Table 10. Statistics of functional annotation of protein-coding genes in *T. rubra* and *A.coerulea*.

Species	Annotation database	Number	Percent(%)
T. rubra	Swissprot	12,770	68.12
	Nr	16,890	90.10
	KEGG	13,385	71.40
	InterPro	16,674	88.95
	GO	7,805	41.64
	Pfam	12,322	65.73
	Annotated	16,898	90.14
	Unannotated	1,848	9.86
A.coerulea	InterPro	24,625	76.87
	GO	13,592	42.43
	KEGG_ALL	30,628	95.61
	KEGG_KO	8,724	27.23
	Swissprot	21,001	65.56
	TrEMBL	30,979	96.70
	NR	30,891	96.43
	Annotated	31,116	97.13
	Unannotated	919	2.87

Supplementary Table 11. Statistics of the non-coding RNA of *T. rubra* and *A.coerulea* genomes.

Species	Type		Copy	Average length(bp)	Total length(bp)	% of genome
T. rubra	miRNA		125	116.00	14,531	0.0050
	tRNA		8,425	75.00	629,943	0.2406
	rRNA		496	98.20	48,709	0.0180
	rRNA	18S	55	189.31	10,412	0.0039
		28S	8	126.50	1,012	0.0004
		5.8S	0	0.00	0	0.0000
		5S	433	86.11	37,285	0.0140
	snRNA		747	128.43	95,935	0.0359
	snRNA	CD-box	43	131.40	5,650	0.0021
		HACA-box	16	185.12	2,962	0.0011
		splicing	676	126.34	85,406	0.0320
A.coerulea	miRNA		65	38.43	2,498	0.0004
	tRNA		2,341	75.19	176,034	0.0306
	rRNA		630	1,741.31	1,097,027	0.1906
	rRNA	18S	187	1,793.33	335,353	0.0583
		28S	183	3,999.16	731,847	0.1271
		5S	260	114.71	29,827	0.0052
	snRNA		39	149.43	5,828	0.0010
	snRNA	CD-box	2	218.00	436	0.0001
		HACA-box	0	0.00	0	0.0000
		splicing	37	145.72	5,392	0.0009
		scaRNA	0	0.00	0	0.0000

411 **Supplementary Table 12. BUSCO evaluation of annotated results.**

412

n=954	Percentages(%)	
	T. rubra	*A. coerulea*
Complete BUSCOs	93.3	88.3
Complete and single-copy BUSCOs	88.4	87.9
Complete and duplicated BUSCOs	4.9	0.5
Fragmented BUSCOs	1.6	4.7
Missing BUSCOs	5.1	6.9

413

Supplementary Table 13. Comparison of genome assemblies of *Turritopsis* and *Aurelia* with published genomic statistics.

Species	***T. rubra***	*T. rubra*	*T.dohrnii*	*T. dohrnii*	***A. coerulea***	*Aurelia* sp1	*A. aurita* （Atlantic）	*A. aurita* (Pacific)
Assembly size (bp)	**266.86**	210.00	390.00	435.92	**566.06**	713.00	377.00	429.00
Contig num	**762**	53,262	68,044	891	**42**	67,005	170,088	213,756
contig N50(bp)	**1,187,606**	3,457	7,666	747,194	**22,395,985**	20k	2,627	2,665
Scaffold num	**329**	9,508	74,829	—	**22**	16,793	2,710	7,744
scaffold N50(bp)	**16,943,197**	71,856	10,419	—	**25,260,120**	124K	1.04M	0.2M
GC Content(%)	**34.26**	34.00	34.50	34.70	**37.34**	32.60	37.10	37.60
TE rate(%)	**47.43**	39.45	50.78	60.35	**73.14**	49.50	44.67	44.03
Complete BUSCOs (%)	**92.40**	88.78	78.88	90.40	**86.40**	—	72.20	49.00
Gene num	**18,746**	9,324	17,468	23,314	**32,035**	29,964	28,625	30,166
Genome coverage	**200×**	96×	95×	219.5×	**120×**	—	90×	90×
Assembly level	**chromosome**	scaffold	scaffold	contig	**chromosome**	scaffold	scaffold	scaffold
Reference	**This study**	Pascual-Torner et al., 2022		Hasegawa et al., 2023	**This study**	Gold et al, 2019	Khalturin et al.,2019	

Supplementary Table 14. GenBank accession numbers of statocyst related PSGs protein sequences of four vertebrate species.

Gene	Species	GenBank accession number
CHSY1	*D. rerio*	NP_997843
	G. gallus	XP_015147744
	M. musculus	NP_001074632
	H. sapiens	AAQ88893
USH2A	*D. rerio*	XP_009291422.1
	G. gallus	XP_015139379.2
	M. musculus	AAZ23164.1
	H. sapiens	KAI4084958.1
CDH23	*D. rerio*	NP_999974.1
	G. gallus	XP_421595.5
	M. musculus	NP_075859.2
	H. sapiens	NP_071407.4
DCTN1	*D. rerio*	XP_021336434.1
	G. gallus	XP_040555015.1
	M. musculus	NP_001185795.1
	H. sapiens	NP_004073.2
CEP83	*D. rerio*	NP_001340860.1
	G. gallus	XP_015139570.1
	M. musculus	NP_084128.2
	H. sapiens	NP_057206.2
KIAA2026	*D. rerio*	XP_005173914.1
	G. gallus	XP_004949130.2
	M. musculus	NP_766424.2
	H. sapiens	NP_001017969.2

Supplementary Table 15. Number of DEGs of the sensory organs compared with control samples in each species (Q<0.01).

Species	Up	Down	Total
T. rubra	1,303	3,335	4,638
C. quinquecirrha	4,796	5,140	9,936
R. esculentum	1,048	413	1,461
A. coerulea	3,698	4,032	7,730

Supplementary Table 16. The sequences of RNAi used in the study.

SiRNA	Number	Sequence (5'-3')
Si-OM	1	CTATCGATCTCACGTTGAA
	2	GGCTACAACAGGCAAACAA
	3	GGCAACGACTTCAAAGGAA
Si-LRR	1	CCTACAACGAAACAGGATA
	2	CCAGACTTTCGAGGAATCA
	3	GGAAACAGTCTCTCAAACA

Supplementary Table 17. RT-qPCR primer sequence of select gene.

Gene name	Sequence (5'-3')
OM	F: TCACGGTTCGATCGCTTTGG
	R: TCCACTGCATCCAGTAGCCT
LRR	F: CCGAGCTTCACCTACAACGA
	R: CGGTGCAAGTTTCATGCCATC

Supplementary Table 18. The Sc-RNA sequencing information of *T. rubra* and *A. coerulea* medusa.

Species	Platform	Data	Number of captured cells	Number of selected cells
T. rubra	10X Genomics	120G	28,607	22,245
A. coerulea	BD Rhapsody	120G	37,671	18,936

Supplementary Table 19. The Sc-RNA sequencing information of five stages of *T. rubra*.

Stage	Platform	Data	Number of captured cells	Number of selected cells
Planula (Pl)	10X Genomics	80G	4,416	4,079
Polyp (Po)	BD Rhapsody	80G	8,647	4,739
Medusa (Me)	10X Genomics	120G	28,607	22,245
Four-leaf structure (Ff)	BD Rhapsody	80G	12,184	8,368
Cyst (Cy)	BD Rhapsody	80G	7,416	5,523

Supplementary Table 20. Sequences of the primers, related to ISH experimental procedures.

Species	Gene name	Gene ID	Sequence (5'-3')
T. rubra	*LOXHD1*	evm.model.Hic_asm_10.1109	F: GGCATTGGTCCTGCATGGTA
			R: GCTGCTTGGTTGATAGTGGC
	USH2A	evm.model.Hic_asm_9.1159	F: GTCAACGTGTCCTGGTCGAT
			R: TCCAGCCCAACATGAAACGA
A. coerulea	*LOXHD1*	Aco27060	F: TTAGCACAGGTGGACTGGT
			R: ACCATCACACGACAAGGTGA
	USH2A	Aco20175	F: ACAGTCGTTGGCTGCTCTAC
			R: AGGTGAGCTTTCTGGTGTCG
	OMs	Aco05836	F: CGATGCCTGACCTAAGAGGC
			R: AAGACGCCTTGTGGCAGATA
	CFAP141	Aco15911	F: TAAGGAACTTGAAGAGCAGTCTGT
			R: CAGTTGAGCTTGCCGAACC